Particle soil crushing: passive detection and interpretation

Ecrasement des grains de sol: détection passive et interprétation

Erdin Ibraim, Sha Luo, Andrea Diambra
Department of Engineering, University of Bristol, sl13796@bristol.ac.uk

ABSTRACT: Soil grain crushing has a significant influence on the performance of the geotechnical systems. However, the mechanics of particle breakage remains one of the most difficult problems in geomechanics. For a bulk of soil grains under loading, one of the ongoing challenges is the prediction of the extent of soil particle crushing and its evolution. While the main goal of a wider research is to investigate the possibility of using Acoustic Emission (AE) technique to characterise the extent and evolution of soil grain crushing, this paper particularly focuses on individual grains under uniaxial compression loading. Insight into the use of AE to characterize the crushing mechanism and signature is gained through testing of individual particles of chalk. For one particle, it appears that the frequency content of the AE recorded signals does not seem to be affected by a particular crushing mechanism, limited fragmentation or critical failure. However, the discrimination between these two mechanisms is given through inspection of the corresponding waveforms and evaluation of parameters like maximum amplitude and energy. Similar size particles also appear to provide good repeatability with similar frequency contents for both crushing mechanisms.

RÉSUMÉ : L'écrasement de grain de sol a une influence significative sur la performance des ouvrages géotechniques. Cependant, la mécanique de la rupture de grains demeure l'un des problèmes les plus difficiles en géomécanique. Bien que le but principal d'une recherche plus large soit d'étudier la possibilité d'utiliser la technique d'émission acoustique (AE) pour caractériser l'étendue et l'évolution de l'écrasement des grains de sol, ce papier se concentre particulièrement sur le comportement individuel des grains sous charge uniaxiale. La connaissance de l'utilisation d'AE pour caractériser le mécanisme et la signature de l'écrasement est obtenue par d'essai sur des grains individuels de craie. Pour une particule, il semble que le contenu en fréquence des signaux enregistrés par AE ne semble pas être affecté par un mécanisme particulier, fragmentation limitée ou l'écrasement critique. Cependant, la discrimination entre ces deux mécanismes est donnée par l'inspection des formes d'onde correspondantes et l'évaluation de paramètres tels que l'amplitude maximale et l'énergie. Des particules de taille similaire semblent également fournir une bonne répétabilité avec des fréquences similaires pour les deux mécanismes d'écrasement.

KEYWORDS: Soil grain, crushing, testing, Acoustic Emission, uniaxial compression loading

1 INTRODUCTION

The design of geotechnical systems requires continuum models for soils whose response is the result of the individual particle arrangement, fabric, and interactions. When the confining pressure is sufficiently large, grain crushing can occur and this can have a significant influence on the performance of a wide range of geotechnical structures such as shallow foundations, embankments and dams, railway substructures (Covarrubias 1969). However, the mechanics of particle crushing remains one of the most difficult problems in geosciences. The link between the breakage of particles and the mechanical response of the soil through adequate continuum constitutive models has not been solved entirely satisfactorily.

Acoustic Emission (AE) monitoring technique has been successfully used in various engineering applications. The acoustic emissions are microseismic events that occur on materials - at small sample scale or large structural scale - during loading. The AE events are recorded by a transducer, or an array of transducers and the data can complement other mechanical measurements of stress or strain by providing insight into various internal material phenomena. The AE technique is widely used for the assessment of damage and failure of brittle materials (Dai and Labuz 1997), evaluation of the response of retrofitted reinforced concrete elements (Yuyama et al. 1994), detection of the onset and position of failure in fiber reinforced composite materials (Giordano M. et al. 1998, Bohse 2000, Huguet 2002, Haselbach 2003), monitoring of large bridge structures (Shigeishi et al. 2001). In geomechanics, pioneering work of Koerner and co-workers (Lord and Koerner 1974) and more recently (Chichibu et al. 1989) used the AE technique to assess the stability of soil slopes. Correlations between the characteristics of the acoustic emission in soils subjected to oedometric compression, triaxial testing, cone penetrometer tests, direct shear and deformation properties, including particle crushing have been conducted by Tanimoto et al. (1981), Fernandes et al. (2010) and Wang et al. (2009), Luo et al. (2016, a and b).

Can Acoustic Emission (AE) be used as a passive technique to infer the extent of particle breakage in a soil mass and predict its evolution under loading? While the answer to this question is the object of a wider research, in this paper, insight into the use of AE technique to characterize the particle crushing mechanism and signature is gained through testing of individual soil grains under uniaxial loading. Experimental test results obtained on individual chalk particles are presented.

2 MATERIAL

Chalk particles with an average equivalent area diameter around 2 mm, 5 mm, 6 mm, and between 8 mm and 10 mm have been selected for testing. The equivalent area diameter is the diameter of the circle which has the same area with the projection area of the particle outlet. The particles have been obtained by hammer crushing of chalk blocks extracted from a quarry located in Préfontaines, France (Hu et al. 2011). Prior to testing, the particles have been washed and dried in the oven for 24 hours.

The shape descriptors and the equivalent area diameter, d_a, for an individual chalk particle have been evaluated using an optical 2D microscope. Six microscope images taken from the particle placed in different positions on the microscope set up, as shown in Figure 1a, and the use of a Matlab Image Analysis package (MATLAB 2010) and an averaging procedure allowed the estimation of the particle circularity (ISO 2008), $C = (4\pi A)/P^2$, and irregularity, $IR = d_{imax}/d_{cmin}$, where A and P are the area and the perimeter of the particle projection, respectively, d_{imax} is the diameter of maximum inscribed circle, d_{cmin} is the diameter of minimum circumscribed circle (Figure

1b). Based on the shape classifications proposed by Blott and Pye (2008) and Mikli et al. (2001), the chalk particles tested in this study appear to have moderate to high circularity while their irregularity lies between rectangular and hexagonal shapes (Figure 1c).

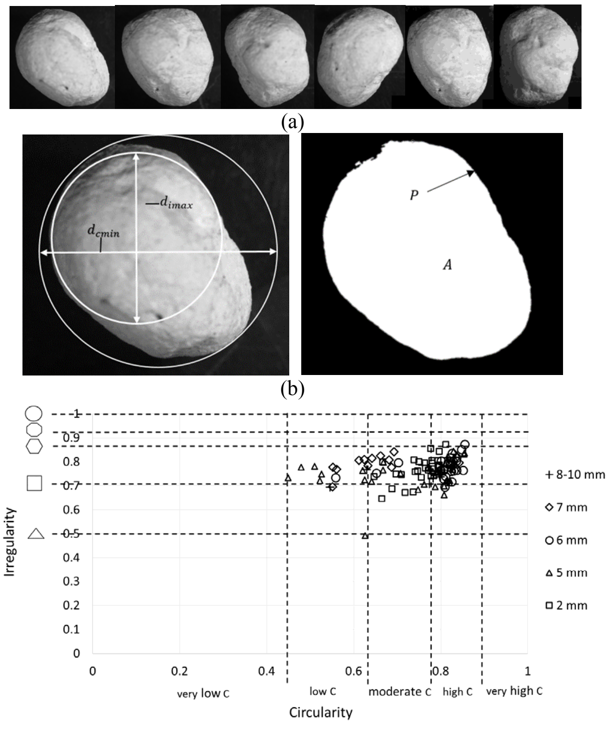

Figure 1. Particle shape characterization: (a) 2D optical microscope images of one chalk particle; (b) definition of some parameters used for shape characterization; (c) shape description of all the chalk particles.

3 UNIAXIAL COMPRESSION TEST

The uniaxial compression test on individual particles is conducted using a displacement controlled electro-mechanical loading frame. Each particle is loaded between two rigid steel platens, of which one (top platen) is attached to a fixed loading ram that incorporates an LVDT for vertical displacement measurements and a 5 kN-load cell. The bottom platen moves upwards with a speed of 0.05 mm/min.

During the crushing test, two piezoelectric sensors with a bandwidth between 10 kHz and 1 MHz record the acoustic emission (AE) signals. The first AE sensor (AE 1), which links to channel 1 of the AE acquisition system, is fixed within the steel base platen, just below the particle at a depth of about 1 cm by means of a mechanical system that ensures a constant holding force (Figure 2). The second AE sensor (AE 2), which links to channel 2, is simply placed on the base platen at a distance of about 4 cm from the particle. For both sensors, silicon grease is also used as a coupler.

During the crushing test, the resulting vertical force and vertical displacement are recorded, while the AE system allows the acquisition of the acoustic bursts recorded at a rate of 1 MS/s and with a fixed 30dB environmental laboratory detection threshold. The set up testing system is completed by a video camera focused on the particle which establishes the connection between the observed particle crushing patterns, force-displacement response and the AE activity.

For each particle size group, the crushing test has been conducted on a sufficient number of particles to account for the inherent variability of the mechanical properties. However, in this paper the discussion of the results will focus more on one size group.

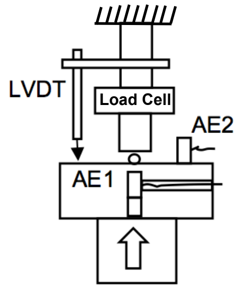

Figure 2. Diagram of loading system

Figure 3 shows the force-displacement relationships recorded during uniaxial compression tests on five chalk particles from the 8 to 10 mm group size. The force-displacement curves are not smooth and at various displacement levels show relatively small but clear decreases in load. These load drops are an indication of limited fracturing mechanism (E) which is generating small fragments from the main particle body. It is also interesting to notice that in the vicinity of the contacts between the particle and the rigid top and bottom steel platens, local material collapse and compaction sometimes accompanied by local crushing are occurring in the initial stages of the loading (Figure 4b). The local material compaction and crushing precede, in general, the limited particle fracturing and generate a low rate response of the axial load as can be observed in Figure 3, where these effects are more pronounced for two of the particles. X-ray tomography tests of some of the chalk grains conducted before testing reveal a material with a very porous structure, localized voids and internal fractures (Figure 5). Major splitting of the chalk particles causing the critical failure (F) occurred at later stages of the test (Figure 4c) and the maximum critical failure force, F_c, recorded. The high variability of the internal structure of the chalk material may also explain the scatter of the recorded critical forces for the particles in one size group. However, the critical force, F_c, data and the corresponding critical tensile stress, σ_F, for all the particle sizes fit well within the uniaxial compression test results obtained by Hu (2009) on the same material and for a wider range of particle sizes (Figure 6a and 6b, respectively). The tensile stress, σ_F, is proportional to the inverse function of the particle diameter squared and in this study is defined following Jaeger (1967) as: $\sigma_F = F_c/d^2$, where d is taken equal with the equivalent particle area diameter, d_a.

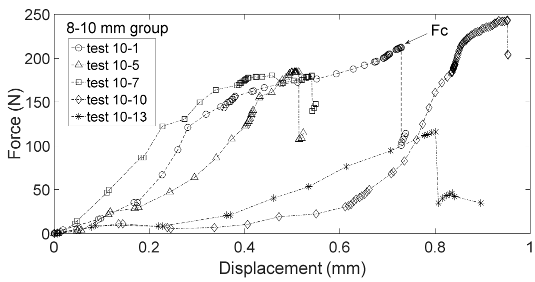

Figure 3. Uniaxial compression of chalk particles: force-displacement response

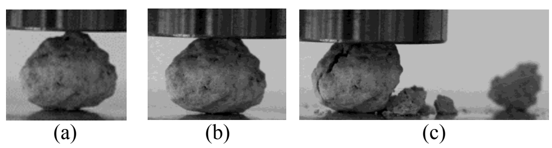

Figure 4. (a) Chalk particle in the experimental set up; (b) initial stage of loading; (c) critical crushing point

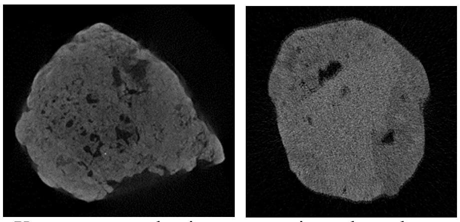

Figure 5. X-ray tomography images: sections through two particles

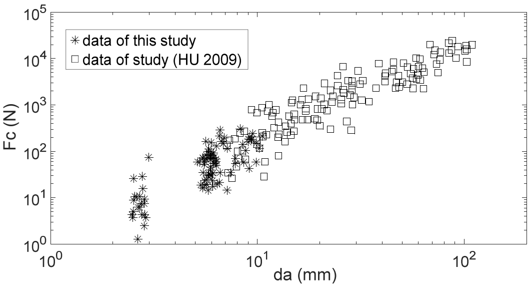

(a)

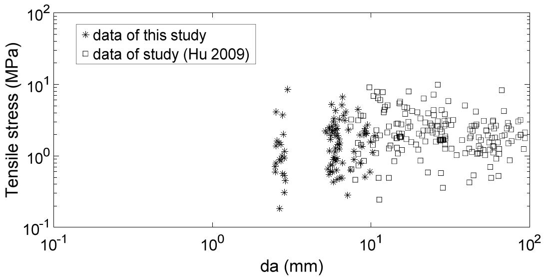

(b)

Figure 6. (a) Relation between the critical failure force, F_c, and particle size, d_a; (b) Relation between the critical tensile stress, σ_F, and particle size (d_a). Data from this study and from Hu (2009).

The probability of survival of a chalk particle of size d_a under tension as a function of normalised critical tensile failure stress (Weibull 1951) is given by:

$$P_s(d_a)=\exp\left(-\left(\frac{\sigma_F}{\sigma_o}\right)^m\right) \quad (1)$$

Where σ_o is a characteristic stress where 37% of the particles survive and m is the Weibull modulus which gives an indication of the data scatter. Figure 7 shows the values of the Weibull modulus for each chalk particle group size within a range between 1 and 4.

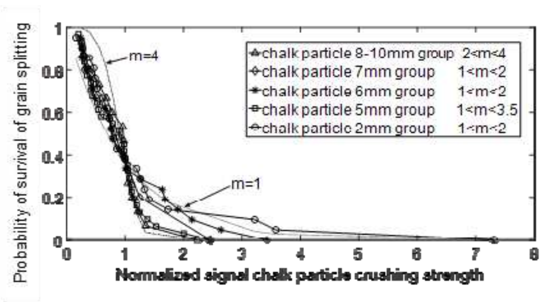

Figure 7. Weibull distributions for the all tested chalk particles

4 ACOUSTIC EMISSION

Typical acoustic emission activity detected during the uniaxial loading test of a chalk particle is illustrated in Figure 8a where the calculated Energy (integral of the rectified voltage signal over the duration of the AE signal) of each recorded AE event is superimposed over the vertical force response. The final crushing point is very visible in the AE records, characterized by a pronounced Energy peak. The maximum amplitudes of AE signals during the AE hits are shown in Figure 8b. Again, the highest maximum amplitude is recorded at the failure crushing point (F) and its magnitude is a few order of magnitude larger than the maximum values recorded for other limited fracturing phenomena (E).

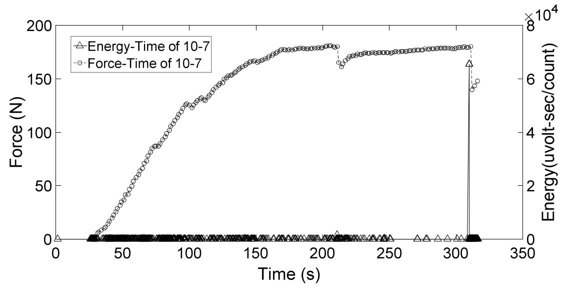

(a)

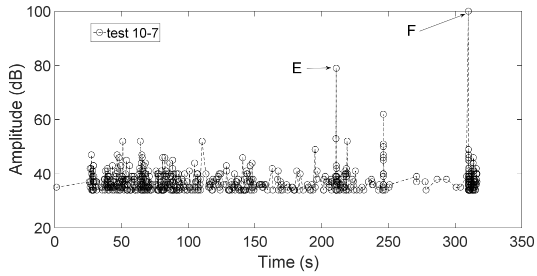

(b)

Figure 8. Test 10-7: (a) Force - Time - (AE) Energy; (b) (AE) Amplitude - Time

Upon particle breakage, and based on the video recordings, the main AE events corresponding to various particle crushing mechanisms (E and F) are isolated. As an example, Figure 9a shows the AE waveform recorded for a 10 mm chalk particle (results shown in Figure 8) at a limited fracturing event E, while Figure 9b shows the AE waveform recorded at the failure crushing point F. The shape of the burst signals represents a typical characteristic of material fragmentation.

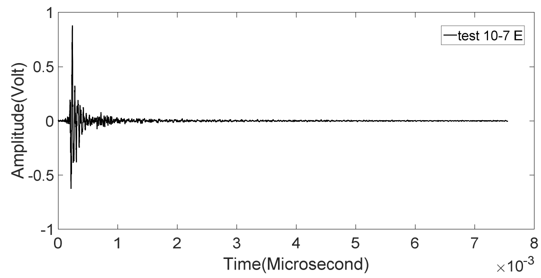

(a)

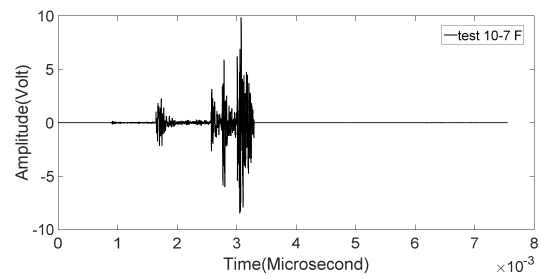

(b)

Figure 9. AE waveforms, test 10-7: (a) event (E); (b) event (F)

The analysis of the AE signals in the frequency domain is based on Welch's power spectral density estimate method (Welch 1967) and was conducted using Matlab software package (MATLAB 2010). The power spectra density estimates of the AE signals for the E and F type events (data for the particle shown in Figure 8) are presented in Figure 10a. Clear frequency peaks are identified in the normalised power spectra densities over a frequency range from 10 kHz to 30 kHz, and they appear to match for these two particularly events, especially the first frequency having the highest amplitude peak at about 12 kHz. Analytical estimation of the fundamental frequency of a spherical particle under the vertical top and bottom fixed kinematic constraints gives a fundamental frequency of about 18 kHz for a shear wave velocity around 700 m/s. A good much of the peaks in the normalized power spectra densities is also observed for the E type events corresponding to two particles with similar sizes (Figure 10b). Figure 10c shows the frequency composition of the signals recorded at the failure crushing point for three 10 mm size particles. While the first peak frequency matches for all three signal events, some differences appear for the higher range of frequencies. Explanation of latter still needs to be establish.

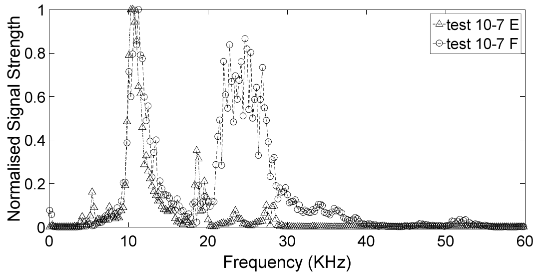

(a)

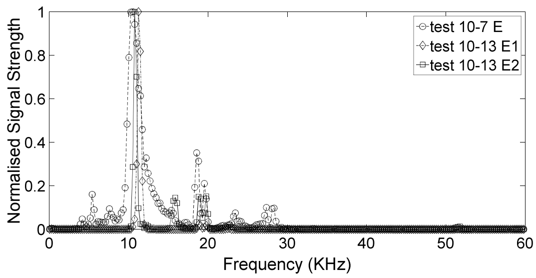

(b)

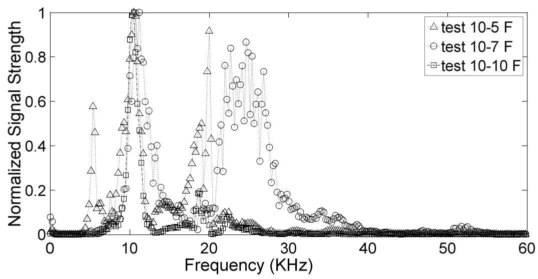

(c)

Figure 10. Frequency content of the AE signals: (a) E versus F for one 10 mm size particle; (b) E type events for two 10 mm size particles; (c) F type events for three 10 mm size particles

5 CONCLUSION

This paper investigates the possibility of using Acoustic Emission (AE) technique to characterize the extent and evolution of soil grain crushing. Insight into the use of AE to characterize the crushing mechanism and signature is gained through testing of individual particles of chalk. For one particle, it appears that the frequency content of the AE recorded signals does not seem to be affected by a particular crushing mechanism, limited fragmentation or critical failure. However, the discrimination between these two mechanisms is given through inspection of the corresponding waveforms and evaluation of parameters like amplitude and energy. Similar size particles also appear to provide good repeatability with similar frequency contents for both crushing mechanisms.

6 REFERENCES

Blott, S. J., & Pye, K. 2008. Particle shape: A review and new methods of characterization and classification. *Sedimentology*, *55*(1), 31-63.

Bohse J. 2000, Acoustic emission characteristics of micro-failure processes in polymer blends and composites, *Compos Sci Technol*, 60, 1213-1226.

Covarrubias SW, 1969. Cracking of Earth and Rockfill Dams, H Harvard University Press: Cambridge, Massachusetts, Vol. 82, 123.

Dai ST, Labuz JF. 1997. Damage and failure analysis of brittle materials by acoustic emission. *J Mater Civil Eng*., 9(4): 200-205.

Fernandes, F., Syahrial, A.I., Valdes, J.R., 2010. Monitoring the oedometric compression of sands with acoustic emissions. *Geotechnical Testing Journal*, American Society for Testing and Materials, 33, 410-415.

Giordano M, Calabro A, Esposito C, D'Amore A, Nicolais L., 1998. An acoustic-emission characterization of the failure modes in polymer–composite materials, *Compos Sci Technol*, 58, 1923-1928.

Haselbach W, Lauke B., 2003. Acoustic emission of debonding between fibre and matrix to evaluate local adhesion, *Composite Science Technology*, 63(15), 2155-2162.

Hu, W., Dano, C., Hicher, P.-Y., Le Touzo, J.-Y., Derkx, F., Merliot, E., 2011. Effect of sample size on the behavior of granular materials. *Geotech. Test. J.* 34(3), 186-197.

Hu, W., 2009. Contribution à l'etude de l'effet d'echelle dans les materiaux granulaires. These Ecole Centrale de Nantes.

Huguet S, Godin N, Gaertner R, Salmon L, Villard D. , 2002. Use of acoustic emission to identify damage modes in glass fibre reinforced polyester, *Compos Sci Technol*, 62, 1433–1444.

ISO 9276-6:2008(E), Representation of results of particle size analysis - Part 6: Descriptive and quantitative representation of particle shape and morphology.

Jaeger, J. C, 1967. Failure of rocks under tensile conditions. *Int. J. Rock. Min. Science*, 4, 219-227.

Lord, A.E., Koerner, R.M., 1974. Acoustic-emission response of dry soils. *Journal of Testing and Evaluation,* 2, 159–162.

Luo, S., Diambra, A., & Ibraim, E. 2016. Application of Acoustic Emission on Crushing Monitoring of Individual Soil Particles in Uniaxial Compression Test. In Proc. of 32nd ECAET: Prague, Czech Republic, Sept, 305-313.

Luo, S., Diambra, A., & Ibraim, E. 2016. Particle crushing: passive detection. 1st IMEKO TC-4. Int. Workshop on Metrology for Geotechnics. Benevento, Italy, March.

MATLAB (The language of technical computing), 7th Ed: The Mathworks Inc, 2010

Mikli, V., Kaerdi, H., Kulu, P., & Besterci, M., 2001. Characterization of Powder Particle. *Methods*, *7*, 22–34.

Shigeishi, M., Colombo, S., Broughton, K.J., Rutledge, H., Batchelor, A.J., Forde, M.C., 2001. Acoustic emission to assess and monitor the integrity of bridges. *Construction and Building Materials*, 15, 35-49.

Tanimoto, K., Nakamura, J., 1981. Studies of acoustic emission in soil. In: Drnevich, V.P., Gray, R.E. (Eds.), *Acoustic Emission in Geotechnical Engineering Practice*, ASTM STP 750, 164–173.

Yuyama S, Okamoto T, Nagataki S, 1994. Acoustic emission evaluation of structural integrity in repaired reinforced concrete beams, *Material Evaluation*, 52(1), 88-90.

Wang, Y., Ma, C., Yan, W., 2009. Characterizing bond breakages in cemented sands using a mems accelerometer. *G. Test. J*, 32, 1–10.

Weibull, W., 1951. A statistical distribution function of wide applicability. *Journal of Applied Mechanics*, Sept., 293-297

Welch, PD. 1967. The Use of Fast Fourier Transform for the Estimation of Power Spectra: A Method Based on Time Averaging Over Short, Modified Periodograms. *IEEE Transactions on audio and electroacoustics*, AU-15, No. 2.